Resource Operators Conference

Faculty of Engineering and Information Sciences

2024

Finite element simulation of fully grouted rock bolts behaviour across varied bore hole diameters

Behshad Jodeiri Shokri

Ali Mirzaghorbanali

Waru Karunasena

Kevin McDougall

Naj Aziz

See next page for additional authors

Authors
Behshad Jodeiri Shokri, Ali Mirzaghorbanali, Waru Karunasena, Kevin McDougall, Naj Aziz, Shima Entezam, Hadi Nourizadeh, Amin Motallebiyan, and Alireza Entezam

FINITE ELEMENT SIMULATION OF FULLY GROUTED ROCK BOLTS BEHAVIOUR ACROSS VARIED BORE HOLE DIAMETERS

Behshad Jodeiri Shokri[1,2], Ali Mirzaghorbanali[1,2], Waru Karunasena[1], Kevin McDougall[3], Naj Aziz [4], Shima Entezam[1,2], Hadi Nourizadeh[1,2], Amin Motallebiyan[1,2], Alireza Entezam[1,2]

***ABSTRACT*:** This paper introduces a finite element (FE) method to simulate the impact of confinement conditions on the axial load-bearing capacity of fully grouted rock bolts. The study utilises a combination of experimental and numerical modelling techniques. For this purpose, two different sizes of steel sleeves were used as confinements with a diameter of 23 mm and 50 mm. The samples were cured after embedding and grouting the bolt for 28 days. Subsequently, pull-out tests were conducted to assess the axial load-bearing capacity of the samples. The results showed a direct correlation between increased confinement diameter and higher values of ultimate pull-out capacities. In addition to the experimental tests, numerical models employing ABAQUS software were developed to simulate and analyse the debonding mechanism along the bolts. By defining the appropriate model geometry, materials properties, boundary conditions, and interactions, the simulation revealed that the debonding mechanism occurred at the bolt-grout interface. Eventually, a comparison between the load-displacement curves derived from the experimental tests and the numerical simulations highlighted the effectiveness of the numerical model in accurately representing the axial load transfer mechanism within the fully encapsulated rock bolts.

BACKGROUND

Changes in the ground's shape cause stress redistribution in the rock mass, leading to the creation of gaps and a decrease in its load-bearing capacity. The safety of workers and equipment, whether in underground spaces or the slope stability, is crucial for engineers. As a result, several applicable techniques, such as applying and installing tendons, have been developed for avoiding, eliminating, or reducing the possibility of catastrophic disasters to make the work environment safer for personnel. Tendons are generally categorised as primary and secondary support systems. The main objective of implementing primary supports, such as rock bolts, is to increase or strengthen the rock mass. In contrast, the secondary types, such as cable bolts, are considered supplementary to the primary ones, particularly in tectonised regions with highly stressed strata. A fully grouted rock bolting system is the most popular and reliable retaining system due to its' simplicity, availability of materials, ease of installation in the field, and cost-effectiveness among various rock bolts. The fully grouted rock bolting system performances can be assessed when they are subject to axial, shear loads and a combination. The fully grouted rock bolts may fail under the axial loading mechanism in one of the five following ways (or potentially the combination of them), failing the bolt element, grout, the surrounding rocks, the interface between bolt-grout, or surrounding rocks and grout (Littlejohn & and Bruce, 1975).

For several decades, many research works have been conducted on studying axial load behaviour due to its importance on the performance of rock bolting systems using experimental studies, such as pull-out, push-out tests in the laboratory or in-situ, analytical studies, and numerical simulations (Aziz et al., 2006; Aziz et al., 2008; Entezam et al., 2023; Gregor, 2023a, 2023b; Jodeiri Shokri et al., 2023; Li et al., 2016; Motallebiyan et al., 2023; Nourizadeh et al., 2023a; H. Nourizadeh et al., 2023). For instance, Aziz and Webb (2003) studied the load transfer mechanism on six different bolt profiles with an encapsulation length of 75 mm, using push tests. The results described that the shearing strength and stiffness were greater in bolts with higher ribs. Aziz et al. (2006) applied several push and pull-out tests to study the effect of the height and spacing of the bolt surface ribs on the behaviour of the bolt/resin systems. After several pull-out and push tests, Aziz et al. (2008) found that the axial bearing

[1] *School of Engineering, University of Southern Queensland, Springfield, 4300, Australia*
[2] *Centre for Future Materials (CFM), University of Southern Queensland, 4350, Australia*
[3] *School of Surveying and Built Environment, University of Southern Queensland, 4350, Australia*
[4] *School of Civil, Mining and Environmental Engineering, University of Wollongong, NSW, 2500, Australia*

capacity is the highest where the profile spacing is 37.5 mm. Li, et al. (2016) carried out a series of pull-out tests to determine the critical embedment length (EL) of fully grouted rock bolts. Feng et al. (2017) conducted a series of pull-out tests to evaluate the anchorage performance of rebar bolts sheathed by various lengths of segmented steel tubes, including 5 cm, 7 cm, 9 cm, 10 cm, and 15 cm which were utilised to simulate layered strata. By conducting several laboratory pull-out tests. Motallebiyan et al. (2023) found that the ultimate bearing capacity increases with an increase in the rib spacing.

The results obtained from the conventional pull-out tests are used for developing analytical and numerical modelling techniques. Li and Stillborg (1999) proposed an analytical model for fully grouted rock bolts assuming the peak shear stress occurs close to the loading point and decreases exponentially towards the free end. Ren et al. (2010) developed an analytical analysis of the fully grouted rock bolts based on a tri-linear bond-slip model. Jalalifar and Aziz (2012) developed a finite element model (FEM) to evaluate the behaviour of materials and their interactions in a fully grouted bolt by applying ANSYS code. Hazrati Aghchai, et al. (2020) developed further the model proposed by Li and Stillborg (1999) by considering the bolt shank failure to determine the load-displacement curve of the bolt's free end analytically. Hadi Nourizadeh, et al. (2023) explored how the mechanical properties of grout and applied confining pressure affect the pull-out performance of fully grouted rock bolts. For this purpose, ABAQUS explicit FE code was employed to simulate the axial behaviour of the fully grouted rock bolts. The results then were used to compare the numerical simulations with experimental pull-out tests, revealing a substantial impact of these factors on the extent of damage caused by the pull-out load in the samples.

The literature review showed that although some identified research studies have been done on applying numerical methods to study the axial load mechanism in the fully grouted rock bolts, it is needed to focus and study the effect of confinement's diameter on the debonding of the fully grouted rock bolts under the axial load. Therefore, the main objective of this paper is to investigate the effect of changing of confinement's diameter with using experimental and numerical studies.

MATERIALS AND METHODS

In order to assess the load-bearing capacity of fully grouted rock bolts under axial loads, a fully grouted rock bolting system was designed, prepared and subjected to pull-out testing using the MTS 100 kN machine at the University of Southern Queensland. The system comprised 16 mm steel reinforcement rebars along with steel confinements measuring 50 mm in length, with two internal diameters including 23 mm and 50 mm. The steel confinement served the purpose of mimicking the surrounding rocks in the setup. All samples were cast and subsequently allowed to cure for a period of 28 days. Pull-out tests were performed using a tensile testing machine at a controlled rate of 1 mm per minute (**Figures 1** and **2**). The results of conducting pull-out tests on rock bolts with different confinements are illustrated in **Figure 3**.

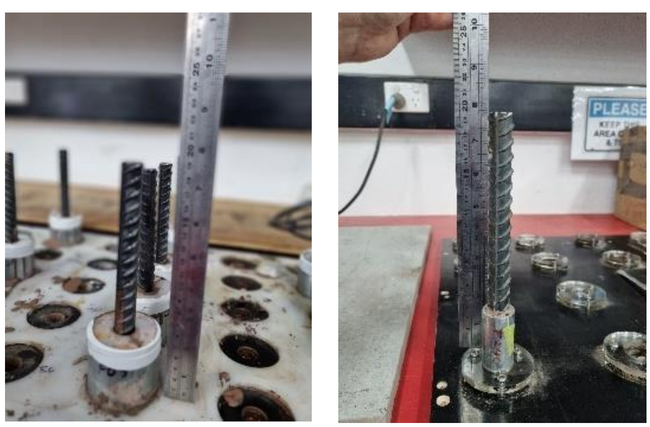

(a) (b)

Figure 1: Samples with ID 50 mm (d) samples with ID 23 mm

(a) (b) (c) (d)

Figure 2: (a) Samples in curing room (b) pull-out test (c) sample with ID 23 mm after the pull-test (d) sample with ID 50 mm after the pull-test

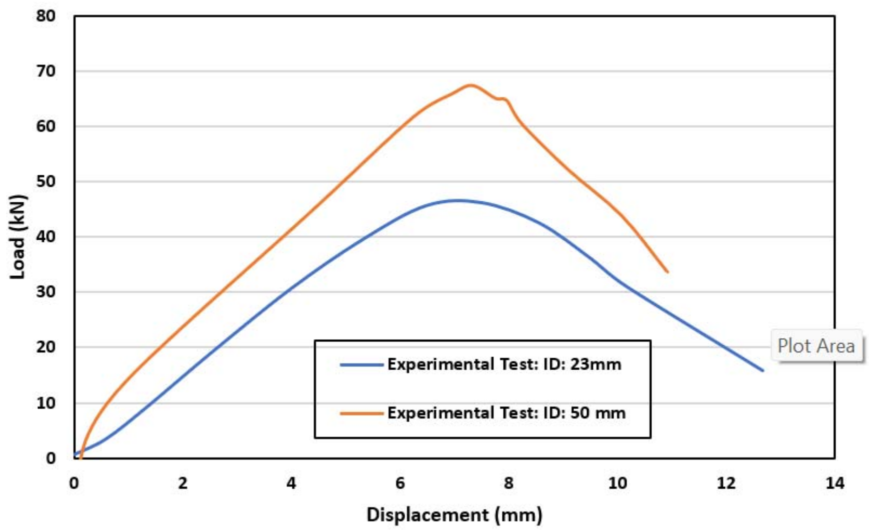

Figure 3: Results of the pull-out test on day 28

NUMERICAL MODELLING

General properties of the model

The simulation of the pull-out tests was conducted using ABAQUS/CAE 6.8, which is also known as Complete Abaqus Environment, serving as the platform for modelling, analysing mechanical components, and visualising finite element analysis results. Its extensive range of material modelling capabilities and customisable features has given it a favoured tool among engineers and researchers. Similar to other FEM software, ABAQUS/CAE encompasses three primary stages:

1. Pre-processing (modelling)
2. Processing (FE analysis)
3. Post-processing (visualising and generating reports based on the analysis outputs)

In this study, following the pull-out tests, a numerical model was generated and validated using the experimental data. The construction of the rock bolt model involves the individual creation of each element, followed by assembly. Notably, due to the extensive time required to run the model, it was segmented into a four-axisymmetric-section model. In this approach, a quarter section was employed for the modelling process. To ensure the simulated model accurately represents the behaviour of a full-sized sample, proper adjustments were made to the boundary conditions.

The initial stage involves constructing the model and defining its geometry. In this study, each component of the model was individually designed based on the geometry of the materials used in the experimental parts. Two distinct materials, steel, and grout were defined and attributed to these components. The bolt consisted of three segments: a 200 mm length cylinder with a 16 mm diameter, along with two distinct ribs-an elongated rib and a spiral rib. These three segments were then combined to form the bolt model as depicted in **Figure 4**.

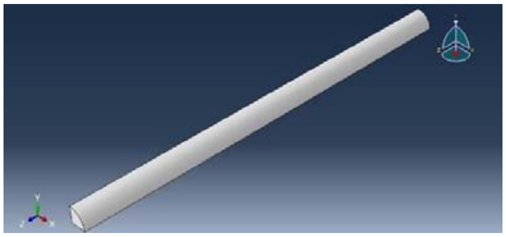

(a)

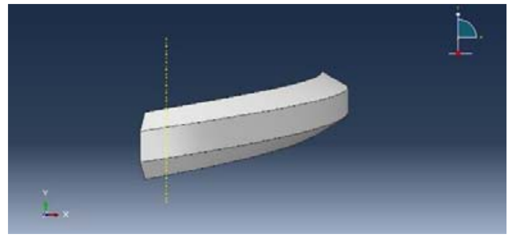

(b)

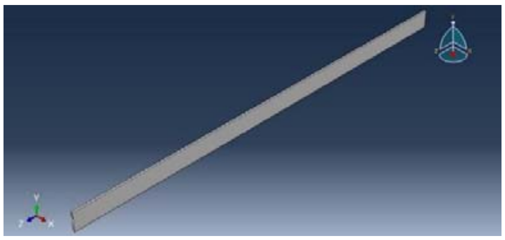

(c)

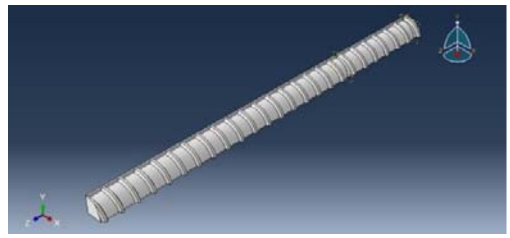

(d)

Figure 4: The process of creating the model (a) rebar without ribs; (b) spiral rib; (c) longitudinal rib, and (d) ribbed bolt

Following the assembly of the bolt components, the next steps involved generating an extruded solid part measuring 50 mm in diameter and 50 mm in height as the confinement and placing the reinforcement rebar in the centre of it (**Figure 5**).

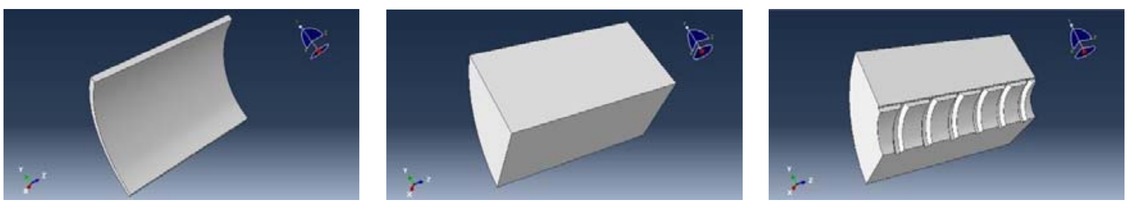

Figure 5: The process of assembly of the model (left) confinement with ID 50 mm; (Centre) grout before excluding the rebar; (Right) grout with the shape of the bolt

Subsequently all three parts joined to shape the model of the rock bolting system (**Figure 6**).

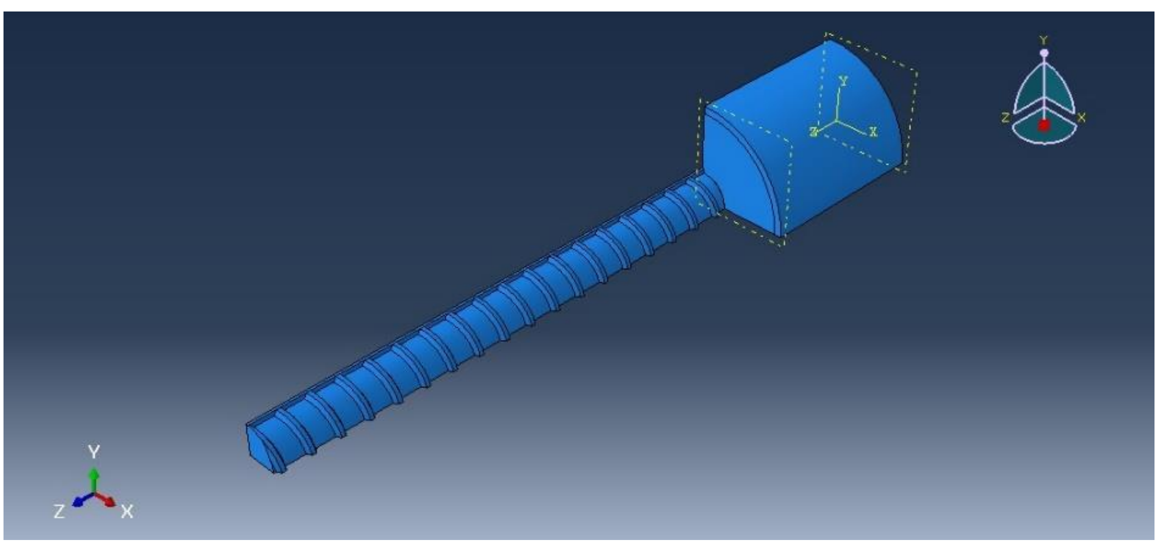

Figure 6: The assembled model of the rock bolt

Material properties

The material properties for both the rebar and grout are detailed in **Table (1)**.

Table 1: Rebar and grout material properties

Variable	Density (kg/m^3)	Elastic	
		Elastic Modulus (GPa)	Poisson's' ratio
Rebar	7800	206	0.3
grout	1889	2.734	0.2

Mesh generation

The inbuilt Abaqus auto-meshing tool was applied along with rebar, grout and confinement (**Figure 7**).

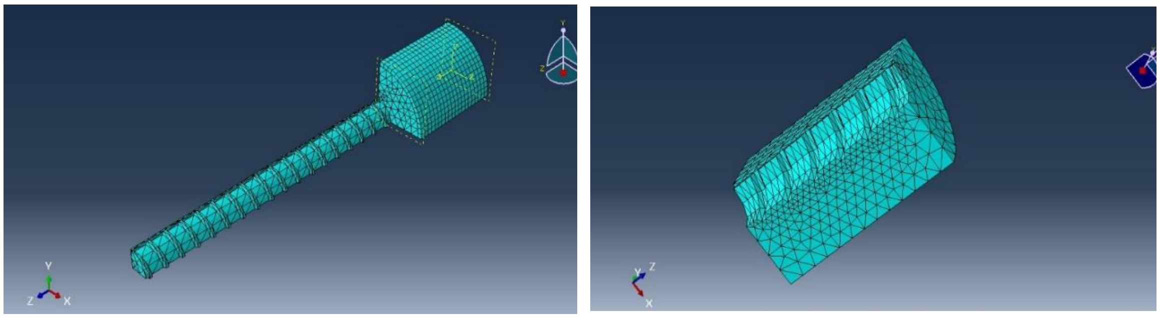

(a) (b)

Figure 7: (a) Meshing along the fully encapsulated rebar; (b) generated mesh on the grout and confinement

Boundary conditions

Since the experimental pull-out tests and previous studies (Yazici & Kaiser, 1992) demonstrated the bolt-grout and grout-confinement interfaces as the most vulnerable component, the interactions between these interfaces were described as **Figure (8)**. The pull-out test procedure consists of securing the confinement and grout while exerting a vertical load onto the contact surface between the steel rebar and the confinement. To simulate this, defining precise boundary conditions is crucial. The confinement and grout were firmly fixed in all directions, with the exception of the bolt's movement within the bolt-grout interface. The ends of the bolt were fixed to prevent any slipping, ensuring stability across all displacement and rotational planes. Loading was applied to the central reference node of the load cell to simulate the testing conditions.

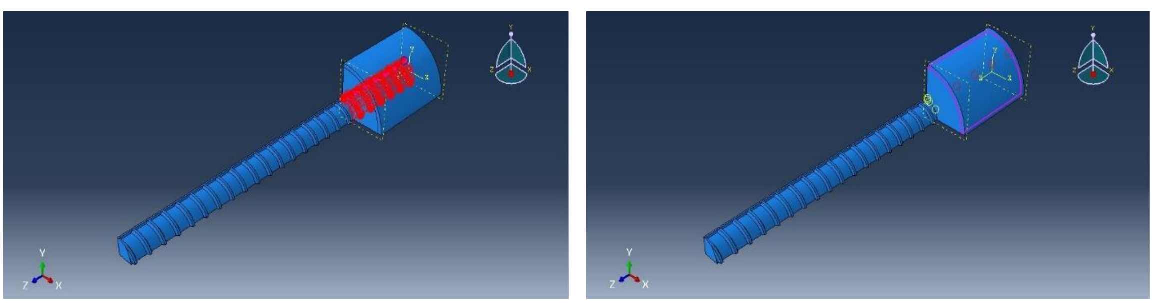

Figure 8: Interactions between (right) bolt-grout and (left) grout-confinement

Simulation the model

Despite opting for a dynamic explicit model for analysis, a mass scaling approach was employed to ensure a valid test. The natural time scale was disregarded due to the simulation involving rate-independent behaviour. The criteria for quasi-static mass scaling can be found in **Table 2**.

Table 2: Quasi-static mass scaling setting

Region	Type	Frequency/Interval	Factor	Target time increment
Whole Model	Target time Inc.	Beginning of step	None	1e-5

RESULTS

The results of the axial loading of the fully encapsulated rock bolt with the confinement with internal diameter of 50 mm were illustrated in **Figures 9** and **10**. **Figure 9** distinctly indicates that debonding took place at the bolt and grout interface. The load-displacement diagram from the pull-out test is depicted in **Figure 10**, demonstrating a peak pull-out capacity of 62 kN. With comparing the results between experimental tests (**Figure 3**) and numerical modelling, it became evident that the numerical model effectively simulated the axial loading mechanism of fully encapsulated rock bolts (**Figure 10**).

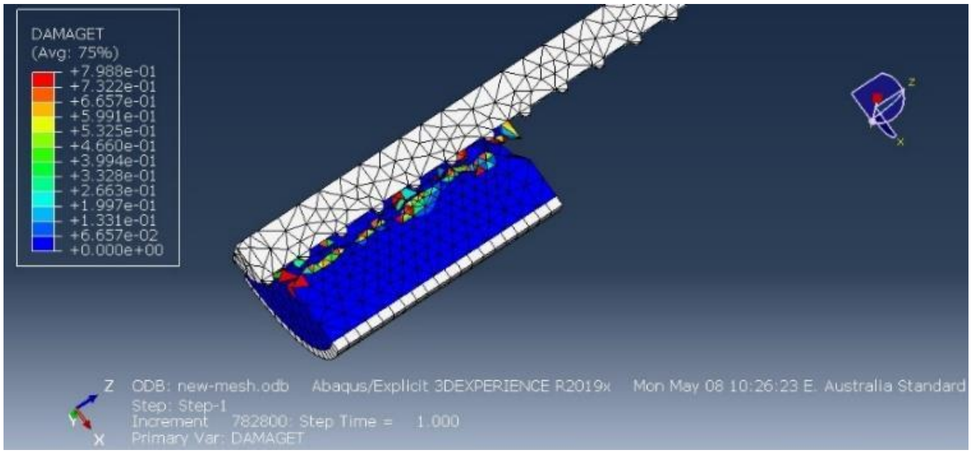

Figure 9: Debonding occurred bolt-grout interface

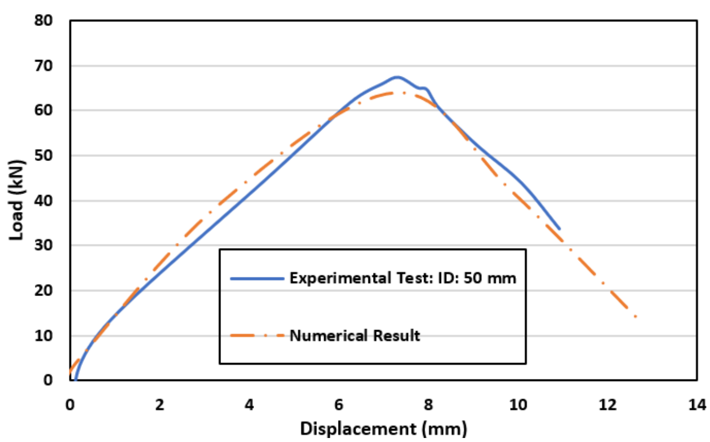

Figure 10: Comparing the results of the experimental tests and the numerical model (Internal diameter of the confinement is 50 mm)

As seen the outcome of the numerical model is in good agreement with the results of the experimental tests. Consequently, the model was successfully recreated for the rock bolting system featuring an internal diameter of 23 mm (**Figure 11**).

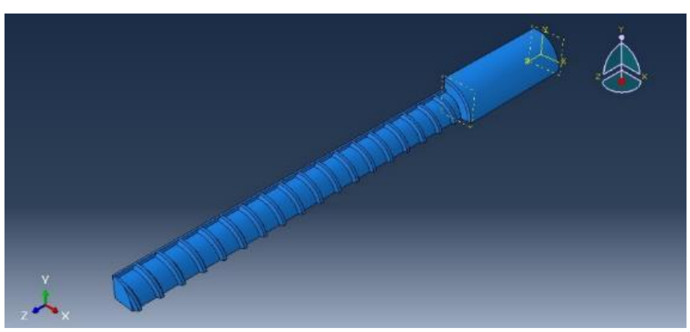

Figure 11: Schematic model of the rock bolt with the ID of 23 mm

Figure 12 displays the fully grouted rock bolt both before and after undergoing the pull-out test. In **Figure 12(b)**, it is apparent that debonding took place at the interface between the bolt and grout which has been already shown as the primary failure mode of the system through the experimental pull-out tests. The load-displacement diagram captured during the pull-out test of the specimen with a 23 mm confinement, demonstrating an ultimate bearing capacity of 47 kN. **Figure 13** demonstrates a notable alignment between the outcomes derived from the numerical model and those obtained through experimental testing.

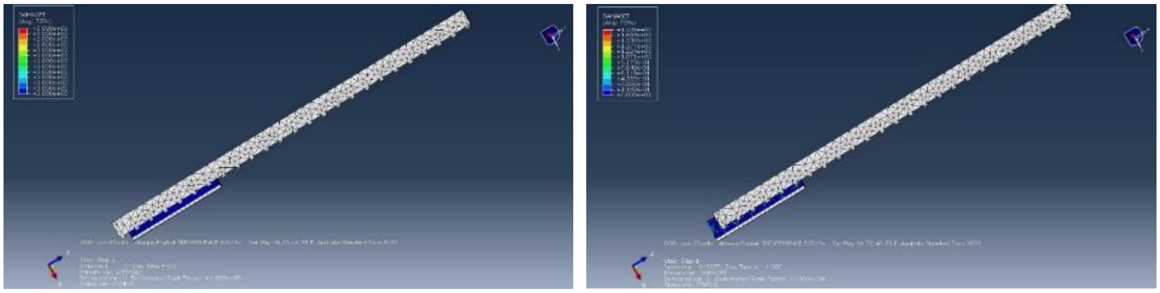

Figure 12: Pull-out model test (a) before running the test, (b) after running the test

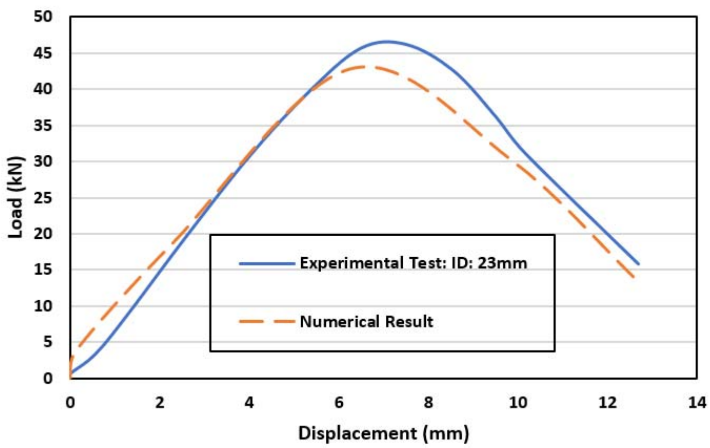

Figure 13: Comparing the results of the experimental tests and the numerical model (Internal diameter of the confinement is 23 mm)

CONCLUSIONS

This study examined the influence of varying confinement diameter on the axial load capacity of fully grouted rock bolts through FE analysis. Two distinct confinement diameters were selected for evaluation. Initially, experimental tests were conducted to generate data for the numerical model simulation. The subsequent comparison between experimental and numerical findings revealed strong concurrence. Further validation was achieved by modifying the grout confinement diameter in the numerical model, consistently demonstrating alignment with experimental outcomes. Also, the numerical results showed that debonding at the bolt/grout interface is the main failure mode of the bolting systems.

REFERENCES

Aziz, N., Jalalifar, H., Concalves, J., 2006. Bolt surface configurations and load transfer mechanism Proceedings of the 2006 Coal Operators' Conference, Wollongong. https://ro.uow.edu.au/coal/51.

Aziz, N., Jalalifar, H., Remennikov, A., Sinclair, S., reen, A., 2008. Optimisation of the bolt profile configuration for load transfer enhancement, 14-15 February 2008. pp: 125-131. Proceedings of the 2008 Coal Operators' Conference, Wollongong, https://ro.uow.edu.au/coal/11.

Aziz, N., Webb, B., 2003. Study of Load Transfer Capacity of Bolts Using Short Encapsulation Push Test Proceedings of the 2003 Coal Operators' Conference, Mining Engineering, University of Wollongong, Australia, https://ro.uow.edu.au/coal/162.

Entezam, S., Jodeiri Shokri B, Nourizadeh H, Motallebiyan A, Mirzaghorbanali A, McDougall K, Aziz N, Karunasena, K., 2023. Investigation of the effect of using fly ash in the Grout mixture on performing the fully grouted rock bolt systems Proceedings of the 2023 Resource Operators Conference, Wollongong, https://ro.uow.edu.au/coal.

Feng, X., Zhang, N., Li, G., Guo, G., 2017. Pullout Test on Fully Grouted Bolt Sheathed by Different Length of Segmented Steel Tubes. Shock and Vibration, 2017, 1-16. https://doi.org/10.1155/2017/4304190

Gregor, P., Mirzaghorbanali, A., McDougall, K., Aziz, N., Jodeiri Shokri, B., 2023a. Investigation shear behaviour of fibreglass rock bolts reinforcing infilled discontinuties for various pretension loads. Canadian Geotechnical Journal. https://doi.org/https://doi.org/10.1139/cgj-2022-0619

Gregor, P., Mirzaghorbanali, A., McDougall, K., Aziz, N., Jodeiri Shokri, B., 2023b. Shear Behaviour of Fibreglass Rock Bolts for Various Pretension Loads. Rock Mech Rock Eng. https://doi.org/https://doi.org/10.1007/s00603-023-03474-1

Hazrati Aghchai, M., Maarefvand, P., Salari Rad, H., 2020. Analytically Determining Bond Shear Strength of Fully Grouted Rock Bolt Based on Pullout Test Results. Periodica Polytechnica Civil Engineering, 1-11. https://doi.org/10.3311/PPci.15195

Jalalifar, H., Aziz, N., 2012. Numerical simulation of fully grouted rock bolts. In (pp. 607-640). INTECHOPEN. https://doi.org/http://dx.doi.org/10.5772/48287

Jodeiri Shokri, B., Entezam, S., Nourizadeh, H., Motallebiyan, A., Mirzaghorbanali, A., McDougall, K., Aziz, N., Karunasena, K., 2023. The effect of changing confinement diameter on axial load transfer mechanisms of fully grouted rock bolts Proceedings of 2023 Resource Operators Conference, University of Wollongong, Wollongong, Australia, https://ro.uow.edu.au/coal/888/

Li, C., & Stillborg, B., 1999. Analytical models for rock bolts. International Journal of Rock Mechanics and Mining Sciences, 36(8), 1013-1029. https://doi.org/https://doi.org/10.1016/S1365-1609(99)00064-7

Li, C. C., Kristjansson, G., Høien, A. H., 2016. Critical embedment length and bond strength of fully encapsulated rebar rockbolts. Tunnelling and Underground Space Technology, 59, 16-23. https://doi.org/10.1016/j.tust.2016.06.007

Littlejohn, G., and Bruce, D., 1975. Rock-anchors state of the art. Design Ground Engineering Part1, 25-78.

Motallebiyan, A., Nourizadeh, H., Jodeiri shokri, B., Entezam, S., Mirzaghorbanali, A., Aziz N, & McDougall, K., 2023. Effects of rib distances on axial load transfer mechanisms of fully grouted rock bolts Resources Operators Conference, https://ro.uow.edu.au/coal/880/

Nourizadeh, H., Mirzaghorbanali, A., Aziz, N., McDougall, K., Jodeiri Shokri, B., Sahebi, A., Mottalebiyan, A., & Entezam, S., 2023a. Finite element numerical modelling of rock bolt axial behaviour subject to different geotechnical conditions, 2023 Resources Operators Conference, Wollongong, https://ro.uow.edu.au/coal/879/

Nourizadeh, H., Mirzaghorbanali, A., Aziz, N., McDougall, K., Jodeiri Shokri, B., Sahebi, A. a., Mottalebiyan, A., Entezam, S., 2023. Finite element numerical modelling of rock bolt axial behaviour subject to different geotechnical conditions Resource Operators Conference, Wollongong, https://ro.uow.edu.au/coal/879/

Nourizadeh, H., Mirzaghorbanali, A., McDougall, K., Jeewantha, L. H. J., Craig, P., Motallebiyan, A., Jodeiri Shokri, B., Rastegarmanesh, A., & Aziz, N., 2023. Characterization of mechanical and bonding properties of anchoring resins under elevated temperature. International Journal of Rock Mechanics and Mining Sciences, 170. https://doi.org/10.1016/j.ijrmms.2023.105506

Ren, F. F., Yang, Z. J., Chen, J. F., Chen, W. W., 2010. An analytical analysis of the full-range behaviour of grouted rockbolts based on a tri-linear bond-slip model. Construction and Building Materials, 24(3), 361-370. https://doi.org/10.1016/j.conbuildmat.2009.08.021

Yazici, S., Kaiser, P. K., 1992. Bond strength of grouted cable bolts. International Journal of Rock Mechanics and Mining Sciences & Geomechanics Abstracts, 29(3), 279-292. https://doi.org/https://doi.org/10.1016/0148-9062(92)93661-3